Supplement of Atmos. Chem. Phys., 25, 9151–9168, 2025
https://doi.org/10.5194/acp-25-9151-2025-supplement

Atmospheric Chemistry and Physics
Open Access
EGU

Supplement of

Simulated photochemical response to observational constraints on aerosol vertical distribution over North China

Xi Chen et al.

Correspondence to: Ke Li (keli@nuist.edu.cn)

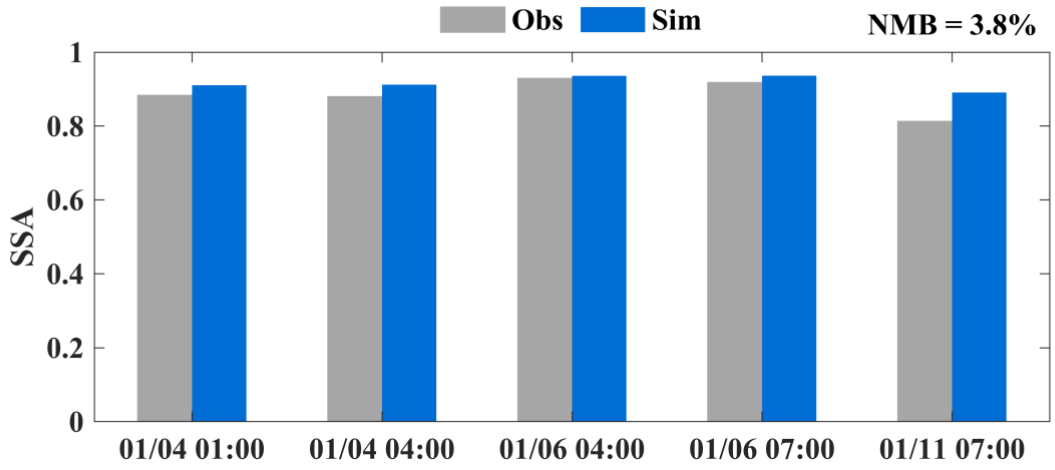

Figure S1: Observed single scattering albedo (SSA) from AERONET and simulated SSA from GEOS-Chem at 440 nm for winter 2017. The observation station is located in Beijing (39.977°N, 116.381°E).

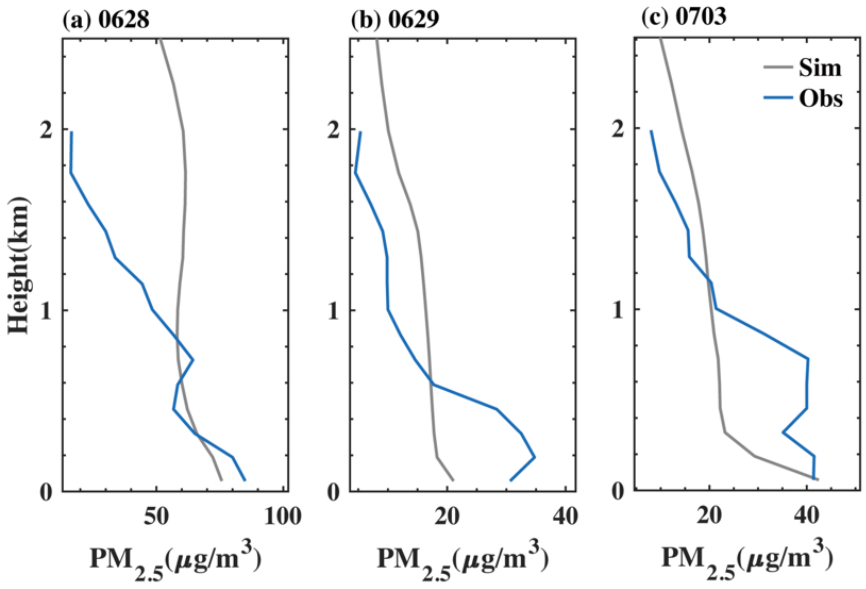

Figure S2: Daily average $PM_{2.5}$ profiles from GEOS-Chem and radiosonde observation on (a) 28 June 2019, (b) 29 June 2019, and (c) 3 July 2019.

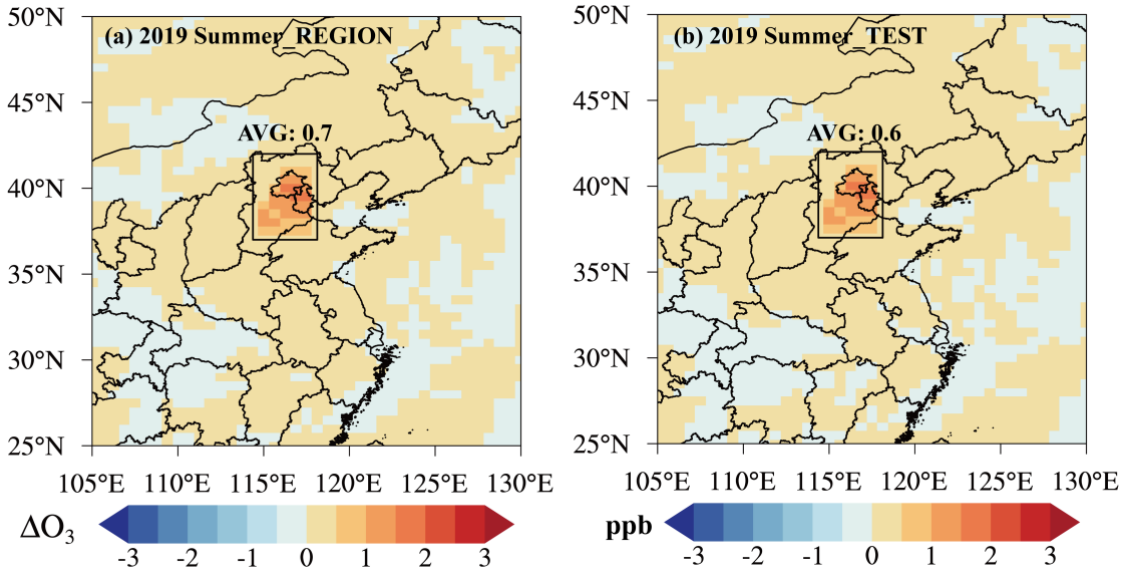

Figure S3: Simulated ozone responses to observational constraints from radiosonde data on aerosol vertical distribution over North China in the summer of 2019. (a) REGION simulation, (b) TEST simulation with the aerosol extinction coefficient in model layer 1 set to be the same as layer 2.

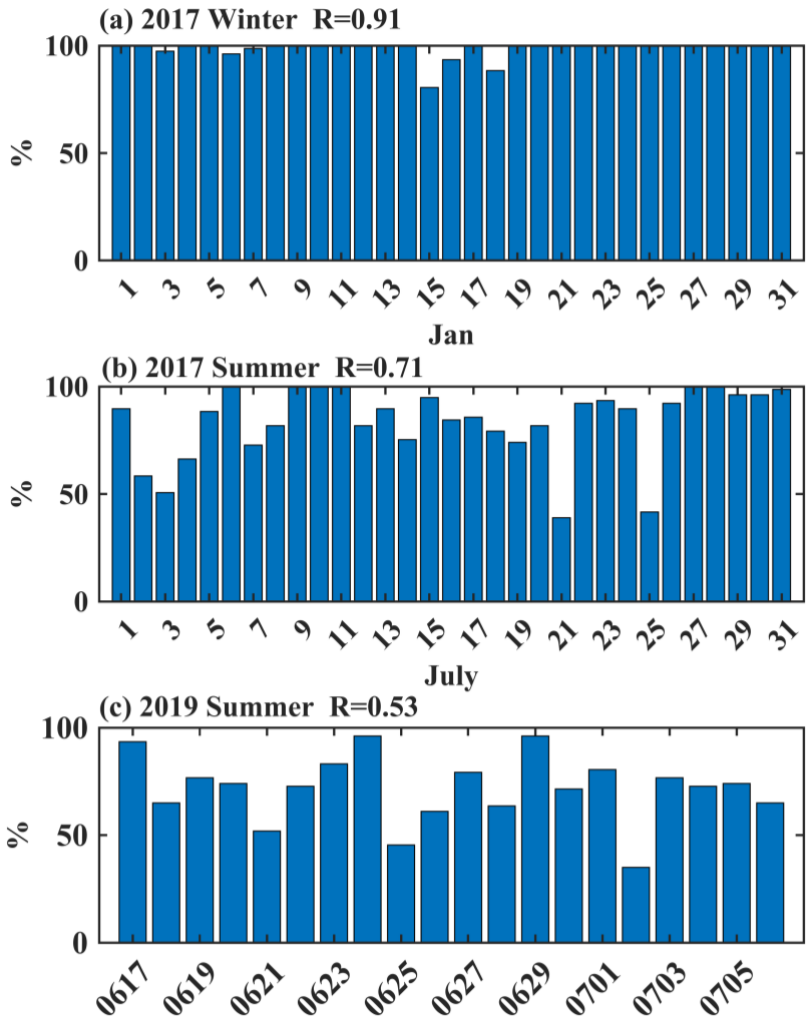

Figure S4: The proportion of grid points in North China with significant correlation with the simulated vertical distribution at observation stations for winter 2017 (a), summer 2017 (b), and summer 2019 (c), respectively. The average correlation coefficient (R) of each simulation period is marked.

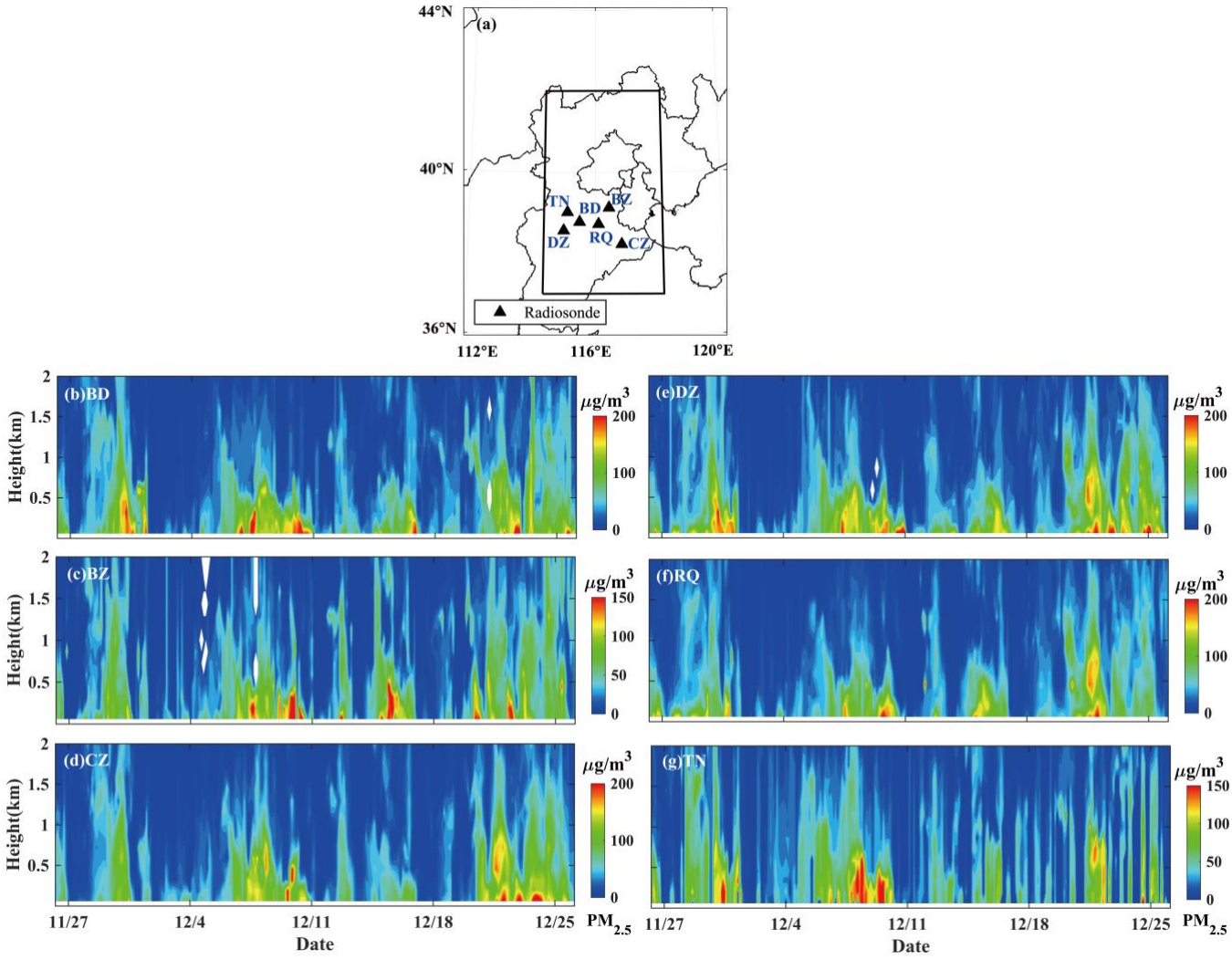

Figure S5: (a) Spatial distribution of radiosonde stations. BD: Baoding; BZ: Bazhou; CZ: Cangzhou; DZ: Dingzhou; RQ: Renqiu; TN: Tuonan. (b–g) Vertical distribution of $PM_{2.5}$ concentrations in model layers from 26 November 2019 to 26 December 2019 at six radiosonde stations.

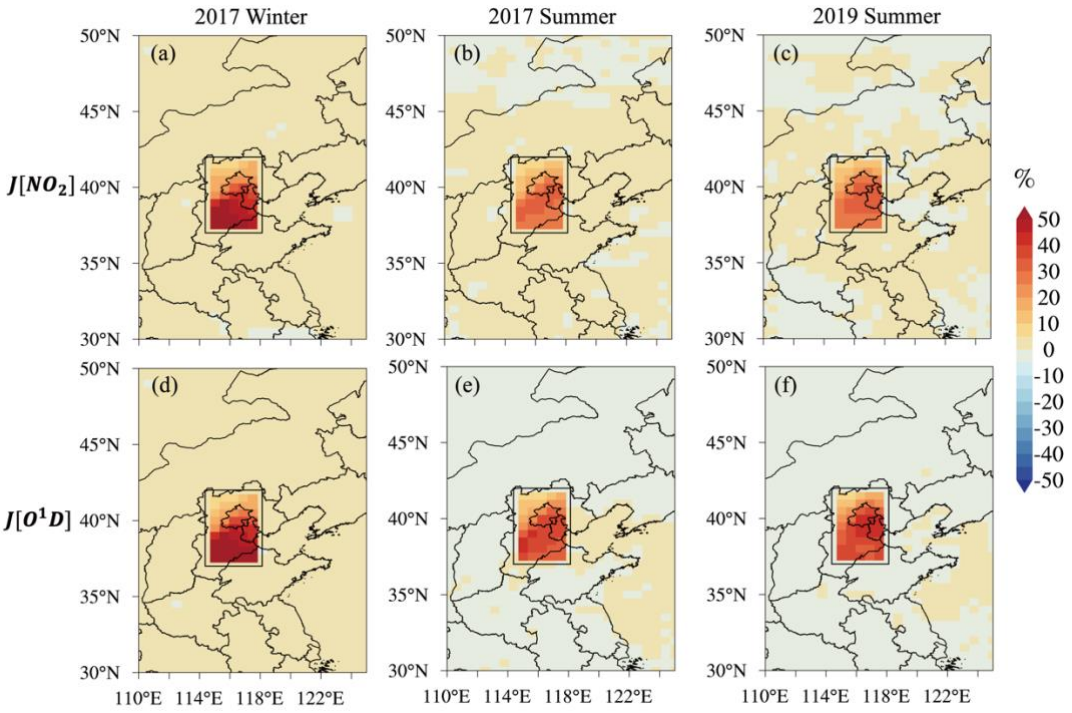

Figure S6: Simulated responses of $\boldsymbol{J[NO_2]}$ and $\boldsymbol{J[O^1D]}$ to observational constraints on aerosol vertical distribution over North China. From left to right are for winter 2017 (a, d), summer 2017 (b, e), and summer 2019 (c, f), respectively. The black rectangle shows the region where vertical distribution modification was performed.

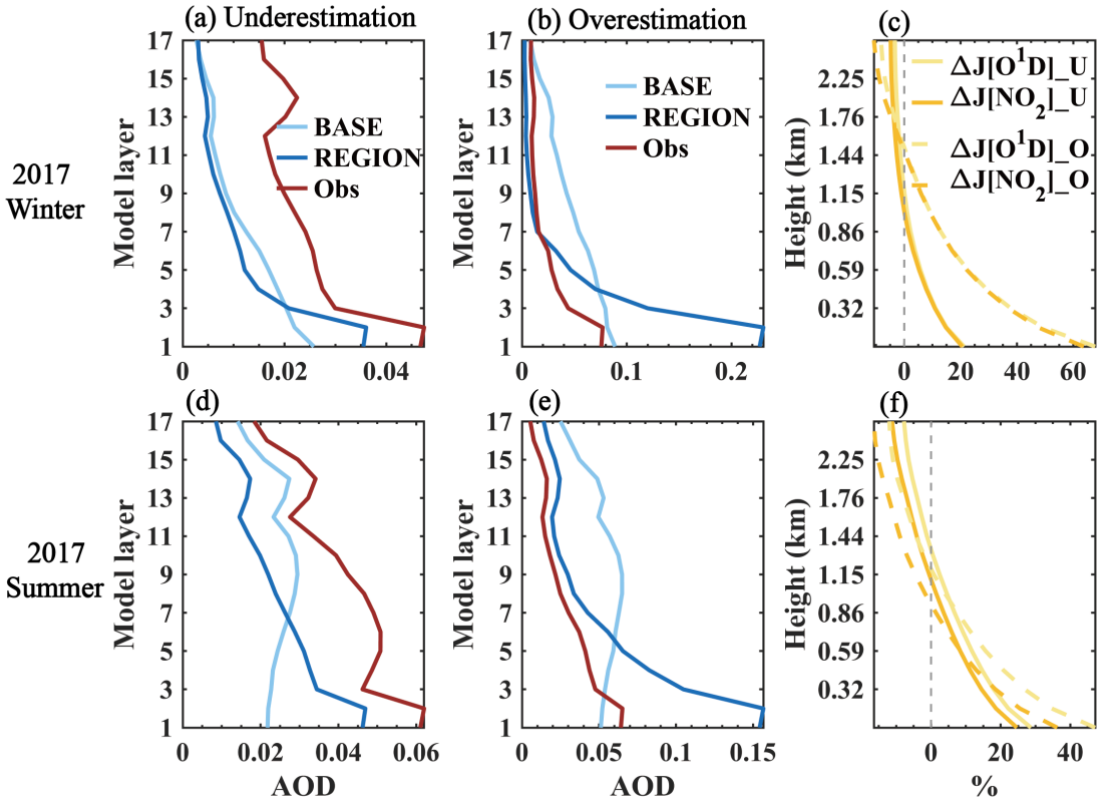

Figure S7: Vertical profiles of average AOD and relative changes of $J[NO_2]$, and $J[O^1D]$ in model layers at lidar station in (a-c) winter 2017 (d-f) and summer 2017. (a, d) AOD profiles with underestimation of total AOD below 3 km. (b, e) AOD profiles with overestimation of total AOD below 3 km. The red, light, and dark blue lines represent observed, BASE simulated, and REGION simulated AOD, respectively. (c, f) Solid lines represent relative changes in photolysis rates with underestimation of total AOD below 3 km, while dash lines represent overestimation.

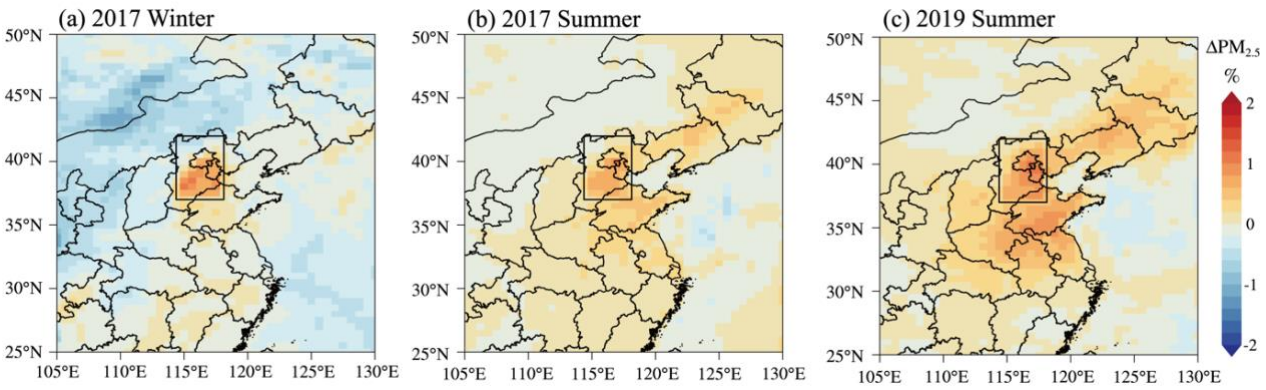

Figure S8: Simulated responses of $PM_{2.5}$ (%) to observational constraints on aerosol vertical distribution over North China. From left to right are for winter 2017 (a), summer 2017 (b), and summer 2019 (c), respectively. The black rectangle shows the region where vertical distribution modification was performed.

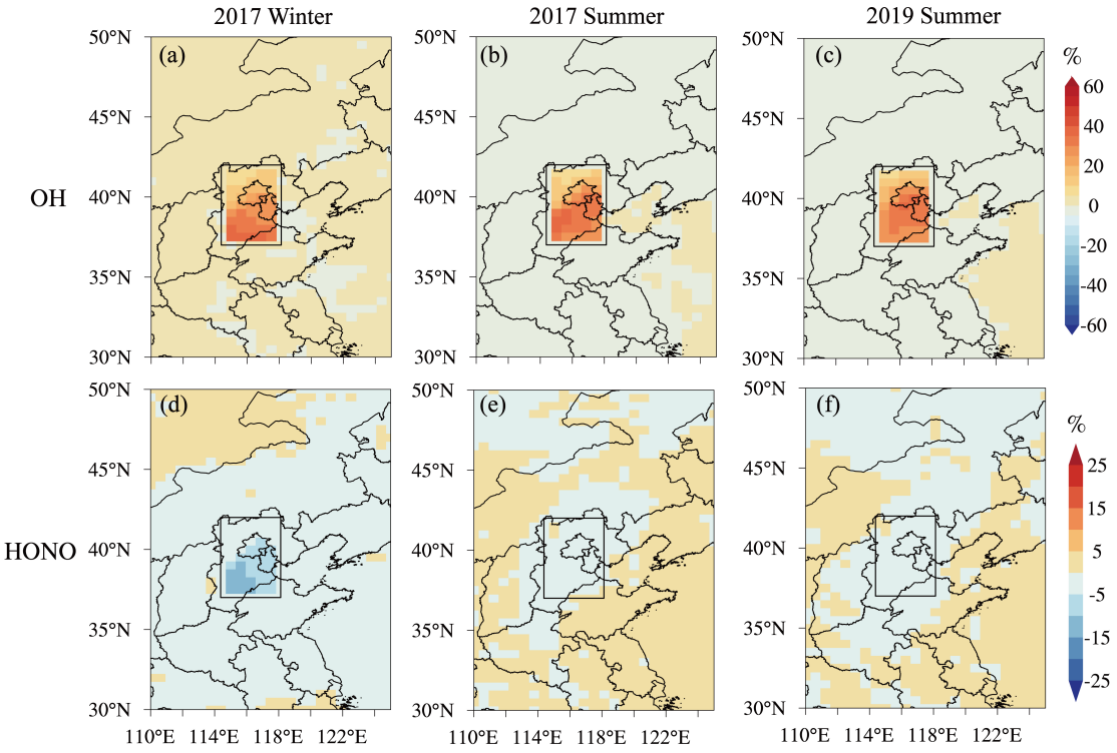

Figure S9: Simulated responses of OH and HONO to observational constraints on aerosol vertical distribution over North China. From left to right are for winter 2017 (a, d), summer 2017 (b, e), and summer 2019 (c, f), respectively. The black rectangle shows the region where vertical distribution modification was performed.

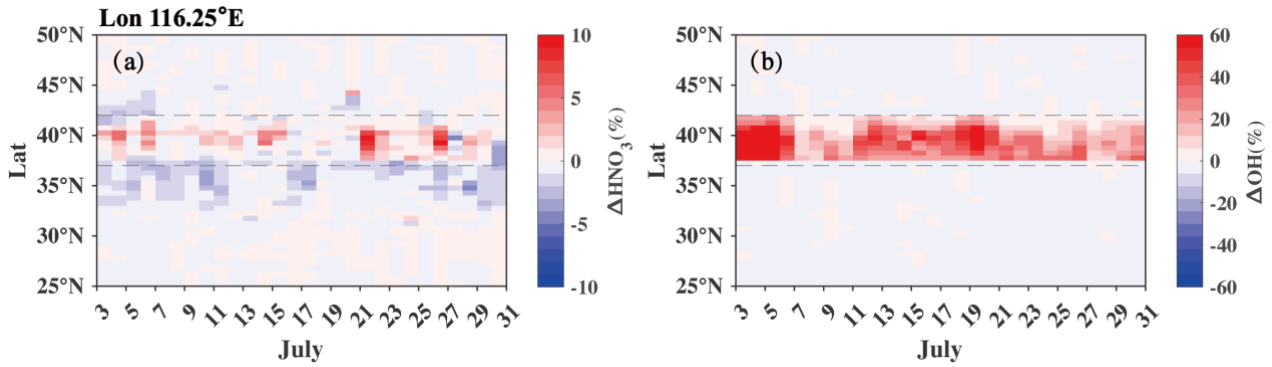

Figure S10: Simulated responses of (a) HNO_3 and (b) OH to observational constraints on aerosol vertical distribution along the longitude profiles of the lidar station in summer 2017. The dotted lines indicate the latitude range of the modified region, and the longitude of the station is marked at the top.

Table S1: Model performance metrics of BASE and REGION simulations for NO_2, ozone, and $PM_{2.5}$ in North China. All statistics were calculated from the average of observation stations in the modified region.

		2017 Winter		**2017 Summer**		**2019 Summer**	
		BASE	REGION	BASE	REGION	BASE	REGION
NO_2	R	0.75	0.76	0.49	0.49	0.61	0.60
	NMB (%)	-22.1	-21.6	-28.3	-29.8	-2.8	-4.8
Ozone	R	0.69	0.65	0.81	0.80	0.84	0.83
	NMB (%)	−24.8	−16.6	44.2	45.9	−0.9	0.4
$PM_{2.5}$	R	0.69	0.69	0.35	0.35	0.80	0.80
	NMB (%)	−4.3	−3.7	21.3	21.9	49.2	49.9

Table S2: The correlation coefficient of observed surface pollutant concentrations at vertical observation stations and all stations in the modified region.

	2017 Winter	**2017 Summer**	**2019 Summer**
Ozone	0.88	0.90	0.95
$PM_{2.5}$	0.70	0.53	0.86

Table S3: List of cases with high planetary boundary layer heights (PBLH) in Figure 5 and low PBLH in Figure 6.

PBLH Type	Date
High PBLH	**2017**: 0703, 0704, 0705, 0709, 0710, 0711, 0712, 0713, 0716, 0717, 0718, 0719, 0720, 0723, 0727, 0729, 0730, 0731 **2019**: 0619, 0620, 0621, 0623, 0624, 0625, 0627, 0628, 0702, 0703, 0704, 0705
Low PBLH	**2017**: 0104, 0105, 0128